

UDK: 628.345; 53.086; 548.73

## Study of Nanosized Hydroxyapatite Material Annealing at Different Retention Times

Miljana Mirković<sup>1\*)</sup>, Ljiljana Kljajević<sup>1</sup>, Suzana Filipović<sup>2</sup>, Vladimir Pavlović<sup>2,3</sup>, Snežana Nenadović<sup>1</sup>

<sup>1</sup>Department of Material Science, "VINČA" Institute of Nuclear Sciences - National Institute of the Republic of Serbia, University of Belgrade, Belgrade, Serbia

<sup>2</sup>Institute of technical sciences of the Serbian Academy of Science and Arts, KnezMihailova 35, Belgrade, Serbia

<sup>3</sup>Faculty of Agriculture, University of Belgrade, Nemanjina 6, Zemun, Belgrade, Serbia

---

### Abstract:

*The aim of the study was to investigate the influence of low heating temperatures with two different retention times to optimize the process for obtaining nanosized hydroxyapatite material that can possibly be used in the fields of biology and pharmacy. Nanosized hydroxyapatite was successfully obtained by wet chemical precipitation. The annealing of the material performed at 300 °C with two different retention times i.e. 3 and 6 hours in air atmosphere. Low annealing temperature with extended retention time was selected in terms to reduce energy consumption. FTIR spectroscopy was used to confirm characteristic vibrational bands of hydroxyapatite samples, and presence of carbonate bands of hydroxyapatite annealed for 3h and 6h. X-Ray powder diffraction analysis were used to examine phase composition, determine the size of unit cells and crystallite sizes, and SEM-EDS methods were used to obtain particle size and arrangement also grain growth morphology and confirmed the presence of calcium, phosphorous oxygen and carbonate peaks. The results show that different retention time has influence on particle growth as well as unit cell parameters and crystallite sizes changes of hydroxyapatite material.*

**Keywords:** Hydroxyapatite; Precipitation; Annealing; X-ray diffraction; SEM-EDS.

---

## 1. Introduction

Hydroxyapatite ( $\text{Ca}_5(\text{PO}_4)_3\text{OH}$ ) is the principal inorganic component of natural bone and teeth. Since it possesses excellent biocompatibility, high-bioactivity, non-toxicity and non-inflammatory properties, this material can be used as a potential biomaterial for hard tissue replacement [1-5]. Hydroxyapatite is crystallographically and chemically similar to the mineralized constituent of hard tissues [6]. Various types of synthesis have been used for preparation hydroxyapatite ceramics, and some of methods of its developing are sol-gel processes [7], hydrothermal synthesis [8] and solid state reaction [9]. Comparing to the above mentioned methods, direct precipitation from aqueous solution method is simpler way for preparing hydroxyapatite powders and also provides the best yield [10, 11]. Advantages of this method include simple equipment, low cost and ability to obtain hydroxyapatite material with large quantity and high purity [1]. Using solution-precipitation technique for processing hydroxyapatite ceramic materials and low temperatures with optimal retention time is

---

\*) Corresponding author: miljanam@vinca.rs

possible to design material with specific morphology, stoichiometry and level of crystallinity [12] comparing to products made by other techniques.

Biological apatite is actually carbonated apatite with partially substitute phosphate groups by carbonate groups in the apatite structure, also hydroxyapatite structure allows a quite number of structural arrangement along *c*-axis [13]. Hydroxyapatite based materials have also been investigated as carriers for various drugs used in treatment of bone tissue disorders, as well as porous carriers suitable for poorly water soluble drugs [14]. Pure hydroxyapatite material is still the most questionable material, but also the most interesting of the calcium phosphate group, especially in terms of thermal treatment. Thermal treatment of hydroxyapatite material is very important since it provides the final microstructural design and chemical composition, and directly governs the mechanical properties as well as the biological behavior [15]. The most commonly used method of powder consolidation is conventional sintering method. Densification of hydroxyapatite compacts normally require sintering at 1000 °C or higher temperatures [16, 17]. However, low temperatures (400-500 °C) are used to preserve the morphology of initial particles and develop microstructures made by nanosized grains. At temperatures below 700 °C particle bonding occurs without densification, specific surface area decreases and porosity imitates properties of bone [2, 15, 18]. There is a lot of scientific studies where the effect of synthesis parameters and calcination temperature on the size, phase composition, and morphology of hydroxyapatite was studied, and similar results were obtained like in our study [1, 19-25] so we wanted to use a temperature slightly higher than the drying temperature and to monitor the changes over time of three and six hours which we considered to be the most optimal in terms of sample preparation.

In the present study lower temperatures with prolonged retention times were used for grain growth and structural behavior of hydroxyapatite material, than it was found in previous research [26]. The aim of this study was to investigate the influence of annealing retention time of nanosized hydroxyapatite. Thermal treatment of previous synthesized material was carried out at 300 °C in air atmosphere with two different optimal retention times 3 and 6 hours in order to obtain influence of retention time to phase and morphology properties of nanocrystalline hydroxyapatite. Namely, due to the energy savings, we used a lower temperature than the ones used so far, as well as for the preservation of the monophasic and nanometric sizes of hydroxyapatite particles. Also, in order to maintain an optimal time, two times were used to compare the results of whether carbonate incorporation occurs during the annealing. Phase, structural and particle morphology properties of untreated-synthesized *e.a.*-HAA and thermally treated at: 300 °C for 3 h *e.a.*-HAb and for 6 h *e.a.*-HAc materials were analyzed.

## 2. Materials and Experimental Procedures

Hydroxyapatite material (HAA) was prepared by wet precipitation method of 0.3 M  $\text{NaH}_2\text{PO}_4 + \text{H}_2\text{O}$  (Kemika, *p.a.*) into 0.5 M  $\text{Ca}(\text{OH})_2$  (Centrohem, *extra pure* > 96 %), 0.5 M solution which was magnetically stirred. Following that, the pH of mixture was adjusted to alkaline medium using  $\text{NH}_4\text{OH}$  (Centrohem, *p.a.* 25 %), at temperature around 80 °C. Obtained hydroxyapatite powder material (HAA) was annealed at 300 °C with retention time of 3 h (HAb) and 6 h (HAc) in air atmosphere. Spectroscopic studies of the obtained powders after synthesis and thermal treatment procedure were carried out in the 4000-500  $\text{cm}^{-1}$  regions using Fourier transforms infrared spectroscopy, in reflectance mode by a Perkin Elmer Spectrum Two FT-IR spectrometer using drift technique. The phase composition of samples and crystallite size evolution were carried out by X-ray powder diffraction (XRD) analysis using Ultima IV Rigakudiffractometer, equipped with  $\text{CuK}\alpha$  radiation, using a generator voltage (40.0 kV) and a generator current (40.0 mA). The range of 5–50°  $2\theta$  was used for all

powders in a continuous scan mode with a scanning step size of  $0.02^\circ$  and at a scan rate of  $5^\circ/\text{min}$ . The PDXL2 program was used to evaluate the phase composition and identification, crystallite sizes and unit cell parameters of all samples [27]. All obtained powders are compared using ICDD data base [28]. For peak identification, crystallite sizes and unit cell parameter refinement PDF card no. 01-073-8418 was used. The morphology of synthesized and thermally treated powders with EDS analysis were examined using Scanning electron microscopy (SEM, JEOL-JSM 6390 LV).

### 3. Results and Discussion

Examination of phase composition, degree of crystallinity and crystallite sizes of synthesized and thermally treated samples were performed by XRD analyses. The obtained hydroxyapatite material corresponds to the PDF card with hexagonal structure data. The XRD patterns of samples HAa, HAb and HAc are shown in Fig. 1.

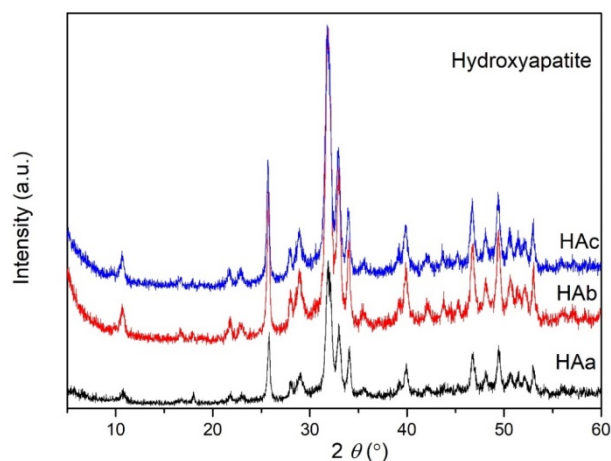


**Fig. 1.** a) synthesized HAa b) HAb treated at  $300^\circ\text{C}$ , 3 h c) HAc treated at  $300^\circ\text{C}$  for 6 h.

According to obtained XRD results, HAa sample has single phase composition  $\text{Ca}_5(\text{PO}_4)_3\text{OH}$ . Diffraction patterns of synthesized sample display broader diffraction peaks of poorly crystalline hydroxyapatite material. Materials obtained by precipitation method have a low degree of order, and obtained results are in correlation with literature data [10]. It is also important to note that the synthesized materials by precipitation method may have a trace of the second phase, which occurred during the precipitation and it is in consistency with applied method. According to results shown in Fig. 1 it is evident that we achieved to synthesize pure HAa material. Fig. 1 also presents hydroxyapatite material (HAb) thermally treated at  $300^\circ\text{C}$  with 3 h retention time in air atmosphere. It is evident that phase composition is the same as untreated material. Also, diffraction peaks which are in range between  $20^\circ$  and  $40^\circ$   $2\theta$  are slightly sharper and have higher intensities compared to HAa. Based on these results it is evident that low temperature treatment of HAb material during 3 h leads slowly to better structural arrangement. Results of HAc material which is treated with 6 h retention time indicate that peaks are much narrower, clearly defined and indicated a better structural arrangement. Based on peak positions and knowledge about crystal structure of hydroxyapatite [6, 13, 16] it is evident that low temperature heating with 3 and 6 h retention time leads to the direction of crystal growth with main reflections.

The average crystallite sizes and unit cell parameters of samples were done in order to see what happens to the structural parameters due to retention time and it is shown in Table I.

**Tab. I** Results of crystallite size and unit cell parameters of investigated HA materials.

Sample	Crystallite size (Å)	Unit cell parameters		
		<i>a</i> (Å)	<i>c</i> (Å)	<i>V</i> (Å <sup>3</sup> )
HAa	94 (3)	9.392(8)	6.907(9)	527.7(6)
HAb	98 (8)	9.378(11)	6.912(12)	526.3(6)
HAc	126 (9)	9.406(8)0	6.920(10)	528.93(7)

As Table I show average crystallite sizes and unit cell parameters of HAa, HAb and HAc. Obviously, it is evident that crystallite size of HAb increase with retention heating time and it has nearly twice the value of crystallite size compared to the initial one. The crystallite size of thermally treated HAc with 6 h retention time is three times higher than the initial crystallite size value. The crystallite size of HAc is significantly larger than that of untreated HAa sample.

It is clear that retention time has significant contribution of crystallite size growth. On the other hand, unit cell parameters indicate growth of unit cell parameters depending on the retention length. The difference between the parameters *c* for the sample HAa and HAb is not significant. However, the parameter *c* in the HAc sample shows a slightly higher value, and it could be related with retention time of material. Namely it is possible that during the 6 h of annealing, carbon from air is incorporated into the structure of hydroxyapatite. The most common case is that it is in the position where the OH group is, *i.e.* in the channel along the axis *c*.

According to some literature data, the exposure to heating of hydroxyapatite in the air atmosphere in a certain period of time due to its structural arrangement of hydroxyapatite can incorporate a carbonate anion along the *c*-axis in structure [13, 29]. FTIR spectroscopy was used also to see if there was the presence of carbonate ions in the structure of hydroxyapatite heated for 3 and 6 h. The FTIR spectroscopy method is a very efficient and useful method for obtaining reliable data on ionic substitutions in the structure. Also, this method is widely used for phosphate minerals testing [30]. FTIR spectroscopy of synthesized HAa, HAb and HAc materials was accomplished in order to support the observations made using XRD. The assumption is that if carbonate is incorporated from the air, these are probably small amounts that can be distinguished by FTIR spectroscopy rather than XRD. In Fig. 2 is shown FTIR spectra of synthesized HAa, HAb and HAc materials and it was compared with the literature data based on which the presence of characteristic vibrations corresponding to apatite was confirmed. For all samples, the doublet at about 601 and 563 cm<sup>-1</sup> corresponds to a triple degenerate bending apatite vibration of the PO<sub>4</sub> molecule, or ν<sub>4</sub> PO<sub>4</sub><sup>3-</sup> vibration [31]. A band at about 960 cm<sup>-1</sup> corresponds to ν<sub>1</sub> PO<sub>4</sub><sup>3-</sup>, which is a non-characteristic apatite vibration. Such "non-apatite" environments indicate the presence of a hydrated layer on the surface of the nanocrystals, and these hydrated layers play a key role in relation to the biological activity of apatite materials [32]. The vibration band at 1028 cm<sup>-1</sup> corresponds to the asymmetric extending PO<sub>4</sub> vibration (ν<sub>3</sub> PO<sub>4</sub>) [31]. FTIR spectra for HAb and HAc samples the band appearing at 870 cm<sup>-1</sup> indicates the ν<sub>2</sub> vibration mode of the HPO<sub>4</sub> or CO<sub>3</sub> group. The strips at about 3400 cm<sup>-1</sup> and 1629 cm<sup>-1</sup> correspond to H<sub>2</sub>O molecules. The bands occurring at about 1461 and 1408 cm<sup>-1</sup> correspond to the vibration of the CO<sub>3</sub> group and indicate a B-type structural arrangement when a portion of the PO<sub>4</sub> group is replaced by a carbonate group [33]. The increased intensity of these band at 867, 1448 and 1413 cm<sup>-1</sup> indicates a clear presence of CO<sub>3</sub><sup>2-</sup> ions in the structure [34, 35].

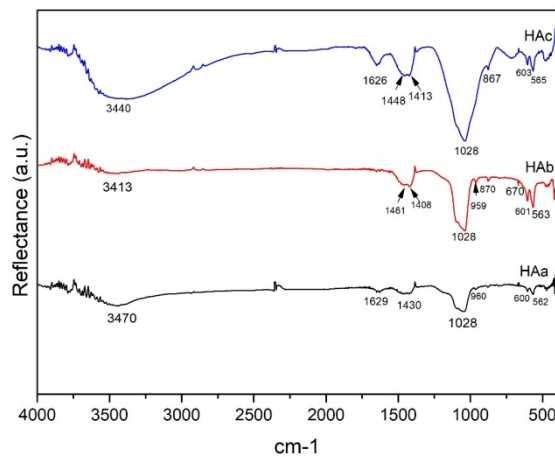


**Fig. 2.** FTIR spectra of HAA, HAB and HAC.

In so far found literature data, this type of carbonate hydroxyapatite is formed when organic compounds are used in the synthesis in which, whereby carbon is not completely pyrolysed during sintering but is dissolved in the hydroxyapatite structure [10]. Since the vibrational bands corresponding to the carbonate vibration mode are not clearly defined in the sample HAC the existence of these vibrations on the FTIR spectrum can be explained by absorbing a certain amount of carbonates from the air during retention time for 6h in air atmosphere.

The results of SEM-EDS analysis of the investigated materials are shown in Figs 3-5. Microphotography of sample HAA, presented in Fig. 3a, is characterized by being mutually adherent and extremely tiny particles, it can be said needle like nano particles. Also, the particles forming irregular shapes of grains, and this agrees with the literature data and the synthesis method used [36]. On Fig. 3b are shown approximate sizes of measured particles and their agglomerates. The particles have needle like shapes less than 20 nm and tend to form grain agglomerates where larger grains approximately have sizes from 200 nm to 1 $\mu$ m, while smaller grains are between 35 nm and 70 nm. SEM results of nano sized material after thermal treatment at 300 °C with 3 h retention time (HAB) are presented in Fig. 4. Fig. 4a shows SEM microphotograph of HAB material, the particles are needle like elongated and they are glued together into agglomerated grains which give each other the appearance of a network. There is an increase in the size and bonding of the grains in sample HAB in comparison to sample HAA. At Fig. 4b are presented approximately values of HAB particles. Particles are about 80 nm while larger grains are up to 2  $\mu$ m and smaller are between 130 nm to 500 nm. Fig. 5 shows microphotographs of HAC powder at 300 °C after 6 h retention time. On Fig. 5a, it can be observed that HAC grains are homogeneously glued into agglomerates up to several microns in size. Based on appearance it can be said that the larger grains are formed from layers of interconnected nanoparticles. Larger grains resemble a partially regular hexahedral shaped and oriented as plate like morphology. There is evident that it is clear that the interspace between the grains is smaller than in the previous two samples and that there is single grain growth on homogenous and nearly uniform surface. This can be explained by the fact that grain growth does not take place at once at the same time throughout the sample, and that retention time has influence on grain growth and homogeneity. At the same temperature during annealing time of 3h the interconnection of initial nanoparticles into larger grains are happening and after 6h tend into agglomerates to form some kind of matrix surface. To observe the size of the aggregated particles in the agglomerate grains taken on a larger magnification, shown of Fig. 5b. According to Fig. 5b it can be said that 6h of annealing leads to rearrangement to larger agglomerates, composed of

grains sizes 90 nm to 250 nm. EDS analysis were done for all tree samples: HAa, HAb and HAC the results are confirmed Ca/P ratio approximately 1.67. Prior to EDS analysis some content of carbon was found in HAb and HAC which confirms XRD and FTIR results that it is possible that carbon incorporation occurred during retention especially for HAC, where carbon content is higher. The results of XRD are in correlation with SEM results, there is better structural arrangement and grain growth due to annealing of hydroxyapatite.

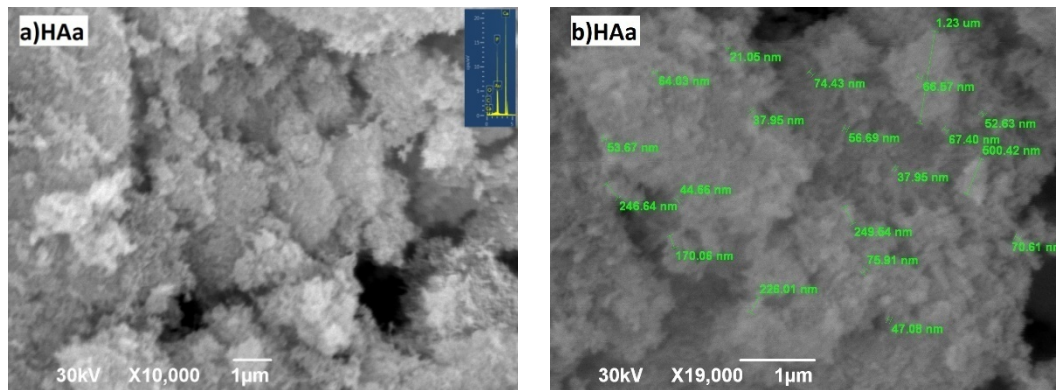


**Fig. 3.** a) SEM-EDS microphotographs of HAa material b) approximate particle sizes of HAa.

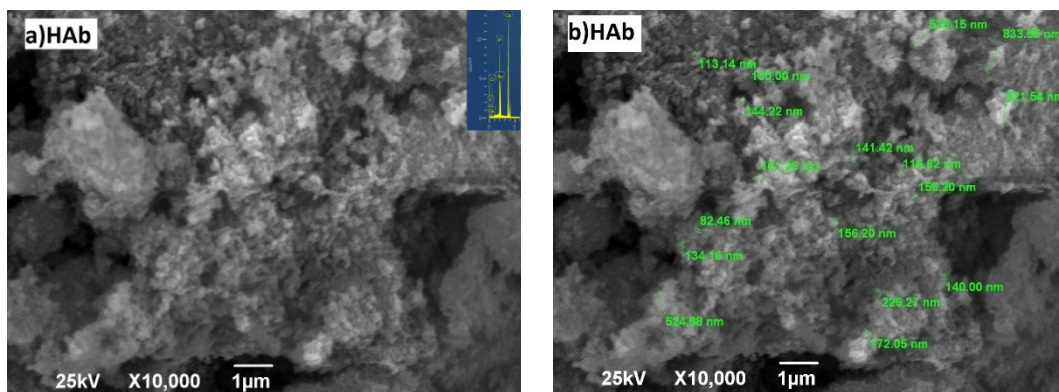


**Fig. 4.** a) SEM-EDS microphotographs of HAb material b) approximate particle sizes of HAb.

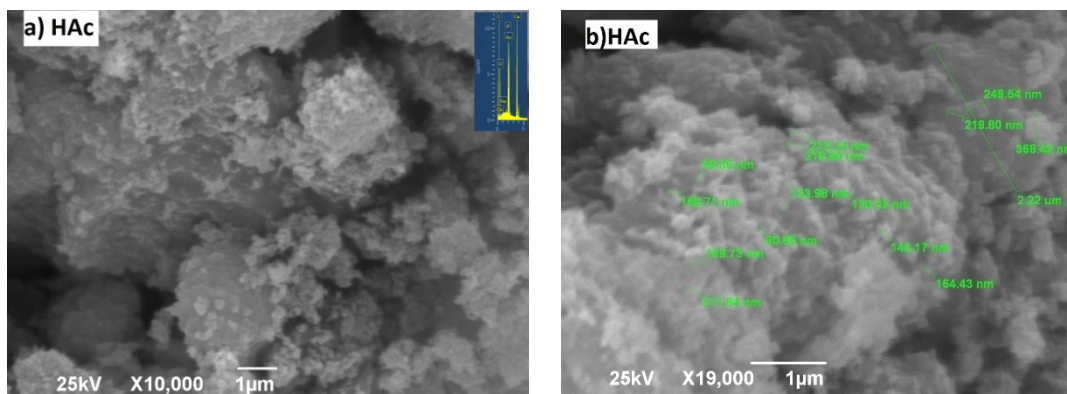


**Fig. 5.** a) SEM-EDS microphotographs of HAC material b) approximate particles sizes of HAC.

The similar grain growth and morphologies of hydroxyapatite grains are achieved by using other methods: changing pH during synthesis, using some additives as polyethylene glycol as template to obtain lamellar and rod shaped hydroxyapatite materials [37, 38]. Due to energy savings and environmental protection low energy annealing method has been more used lately [39, 40]. Artificial hydroxyapatite material to be used as an implant for example bone implant has to have a hollow and reticulate structure and yet the powder needs to remain nanocrystalline and monophasic which we achieved just using prolonged retention time on low temperature treatment. For design of this type of hydroxyapatite material various methods with different additives during synthesis are used. Nevertheless, low temperature heating with a given interval *ea.* the retention of 3 and 6 hours at the same temperature achieved similar targets in comparison to the previously used synthesis [10]. It is a simpler and shorter procedure to obtain specific grain size and specific morphology of powders using low thermal treatment, without altering the chemical composition and phase composition of the desired material.

#### 4. Conclusion

The nanometric hydroxyapatite is successfully synthesized using precipitation method. The results of FTIR spectroscopy confirmed the persistence of vibrations that are specific to hydroxyapatite material, vibrations of carbonate are confirmed for 6h annealed sample-HAc. The results of XRD and EDS analysis confirmed the uniformity of the composition of all examined samples. It can be concluded that low – temperature annealing with different retention times lead to changes in surface morphologies of hydroxyapatite material. Crystallite size grows according to the length of the thermal treatment, also the agglomeration and grain formation of needle like initial particles. SEM analysis confirmed that during the heating process grain growth occurred, but also gave insight into the plate like grain morphology and surface homogeneity with random pore layout. It was found that by changing the retention time of annealing at lower temperatures than previously used it is possible to achieve different grain sizes and shapes, and adjust powder morphology to obtain desired density and pore distribution. It is also obvious that during 6 h of the annealing at 300 °C the hydroxyapatite tends to the carbonate hydroxyapatite composition and structural arrangement. This is cost effective and simple method that does not require any additives, and can be applied in order to obtain Hydroxyapatite material with targeted grain morphology shape, suitable for specific application due consumers' needs.

#### Acknowledgments

Funds for the realization of this work were provided by the Ministry of Education, Science and Technological Development of the Republic of Serbia number 451-03-68/2020-14/200017, and agreement on realization and financing of scientific research work of the Institute of Technical Sciences of SASA in 2020 (Record number 451-03-68/2020-14/200175).

#### 5. References

1. T. P. N. Pham, T. N. Pham, T. P. Vu, H. Thai, T. M. T. Dinh, *Adv in Nat Sci.*, 4 (2013) 1-9.
2. S. J. Kalita, A. Bhardwaj, H. A. Bhatt, *Mat Sci Eng C.*, 27 (2007) 441-449.
3. S. J. Kalita, S. Verma, *Mat Sci. Eng. C.*, 30 (2010) 295-303.

4. H. Zhou, J. Lee, *Acta Biomater.*, 7 (2011) 2769-2781.
5. L. I. Wang, X. F. Wang, C. L. Yu, Y. Q. Zhao, *Sci. of Sinter.*, 47 (2015) 107-112.
6. S. C. Cox, P. Jamshidi, L. M. Grover, K. K. Mallick, *Mat. Sci. Eng. C.*, 35 (2014) 106-114.
7. F. Bakan, O. Laçin, H. Sarac, *Powd Tech.*, 233 (2013) 295-302.
8. M. Sadat-Shojai, M.-T. Khorasani, A. Jamshidi, *J Cryst Growth*, 361 (2012) 73-84.
9. S. Pramanik, A. K. Agarwal, K. N. Rai, A. Garg, *Ceram. Int.*, 33 (2007) 419-426.
10. I. Mobasherpour, M. S. Heshajin, A. Kazemzadeh, M. Zakeri, *J. Alloy. Compd.*, 430 (2007) 330-333.
11. A. K. Nayak, *Int Jour ChemTech Research*, 2 (2010) 903-907.
12. M. Khalid, M. Mujahid, S. Amin, R.S. Rawat, A. Nusair, G. R. Deen, *Ceram. Int.*, 39 (2013) 39-50.
13. R. Zapanta-Legeros, *Nature*, 206 (1965) 403-404.
14. J. Kolmas, S. Krukowski, A. Laskus, M. Jurkitewicz, *Ceram. Int.*, 42 (2016) 2472-2487.
15. E. Champion, *Acta Biomater.*, 9 (2013) 5855-5875.
16. S. Ramesh, K.L. Aw, R. Tolouei, M. Amiriyani, C.Y. Tan, M. Hamdi, J. Purbolaksono, M.A. Hassan, W.D. Teng, *Ceram. Int.*, 39 (2013) 111-119.
17. Đ. Veljovic, E. Palcevskis, P. Uskokovic, R. Petrovic, Đ. Janackovic, *Sci of Sinter.*, 45 (2013) 233-243.
18. M. Sadat-Shojai, M.-T. Khorasani, E. Dinpanah-Khoshdargi, A. Jamshidi, *Acta Biomater.*, 9 (2013) 7591-7621.
19. E. Caponetti, M. L. Saladino, D. F. Chillura Martino, A. Zanotto, *ANP*, 1 (2012) 21-28.
20. Y. M. Z. Ahmed, S. M., EL-Sheikh, Z. I., Zaki, *B Mater Sci*, 38 (2015) 1807-1819.
21. D. R. R. Lazar, S.M. Cunha, V. Ussui, E. Fancio, N.B. de Lima, A.H.A., Bressiani, *Mater. Sci. Forum* 530-531 (2006) 612-617.
22. H.-Y. Juang, M.-H. Hon, *Ceram. Int.*, 23 (1997) 383-387.
23. H. Y. Juang, M. H. Hon, *Biomaterials*, 17 (1996) 2059-2064.
24. S. Raynaud, E. Champion, D. Bernache-Assollant, *Biomaterials*, 23 (2002) 1073-1080.
25. D. Bernache-Assollant, A. Ababou, E. Champion, M. Heughebaert, *J. Eur. Ceram. Soc.*, 23 (2003) 229-241.
26. A. Yelten-Yilmaz, S. Yilmaz, *Ceram. Int.*, 44 (2018) 9703-9710.
27. Rigaku, *PDXL Integrated X-Ray Powder Diffraction Software*, Rigaku, Tokyo, 2011.
28. International Crystallographical Database (ICDD), in: N.S. 12 Campus Blvd, PA 19073, USA (Ed.), USA, 2012.
29. N. Y. Mostafa, H. M. Hassan, F. H. Mohamed, *J. Alloy. Compd*, 479 (2009) 692-698.
30. A. Antonakos, E. Liarokapis, T. Leventouri, *Biomaterials*, 28 (2007) 3043-3054.
31. M. Iafisco, A. Ruffini, A. Adamiano, S. Sprio, A. Tampieri, *Mat. Sci. Eng. C*, 35 (2014) 212-219.
32. D. Grossin, S. Rollin-Martinet, C. Estournès, F. Rossignol, E. Champion, C. Combes, C. Rey, C. Geoffroy, C. Drouet, *Acta Biomater*, 6 (2010) 577-585.
33. M. H. Fathi, A. Hanifi, V. Mortazavi, Preparation and bioactivity evaluation of bone-like hydroxyapatite nanopowder, *Journal of Materials Processing Technology*, 202 (2008) 536-542.
34. O. Frank-Kamenetskaya, A. Kol'tsov, M. Kuz'mina, M. Zorina, L. Poritskaya, *J Mol Struct*, 992 (2011) 9-18.
35. M. E. Fleet, *Biomaterials*, 30 (2009) 1473-1481.
36. H. H. Abo-Almaged, A. A. Gaber, *Mater Today Commun*, 13 (2017) 186-191.
37. P. Mehta, B. S. Kaith, *Int J Biol Macromol*, 107 (2018) 312-321.



38. G. Zuo, X. Wei, H. Sun, S. Liu, P. Zong, X. Zeng, Y. Shen, J. Alloy. Compd, 692 (2017) 693-697.
39. A. Modrić-Šahbazović, M. Novaković, E. Schmidt, N. Bibić, I. Gazdić, C. Ronning, Z. Rakočević, Sci. of Sinter., 52 (2020) 207-217.
40. A. Terzić, L. Pezo, Lj. Miličić, N. Mijatović, Z. Radojević, D. Radulović, Lj. Andrić, Sci. of Sinter, 51 (2019) 39-56.

---

**Сажетак:** Циљ студије био је истражити утицај термичког третмана на ниским температурама са два различита времена задржавања како би се оптимизовао процес добијања хидроксиапатитског материјала наночестичних димензија који би се могао користити у областима биологије и фармације. Наночестични хидроксиапатит је успешно добијен мокрим поступком хемијске титрације. Жарење материјала вршено је на 300 °C са два различита времена задржавања, тј. 3 и 6 сати у атмосфери ваздуха. Ниска температура жарења са продуженим временом задржавања изабрана је у смислу смањења потрошње енергије. Фуријеова трансформација са инфрацрвеном спектроскопијом коришћена је за потврђивање карактеристичних вибрационих опсега узорака хидроксиапатита као и присуство карбоната код хидроксиапатита термички третираних током 3 и 6 сати. Рендгенска дифракциона анализа коришћена је за испитивање фазног састава, одређивање величине јединичних ћелија и величина кристалита, а СЕМ-ЕДС методе коришћене су за добијање величине и морфологије изгледа честица, такође ЕДС методом потврђено је присуство калцијума, фосфора кисеоника и карбоната. Резултати показују да различито време задржавања има утицаја на раст честица, промену параметара јединичне ћелије и величине кристалита нано хидроксиапатита.

**Кључне речи:** хидроксиапатит, титрациона метода, жарење, рендгенска дифракција, СЕМ-ЕДС.

---

© 2020 Authors. Published by association for ETRAN Society. This article is an open access article distributed under the terms and conditions of the Creative Commons — Attribution 4.0 International license (<https://creativecommons.org/licenses/by/4.0/>).

